Estrogen inhibits the apoptosis of spiral ganglion cells in C57BL/6J mice with presbycusis by downregulating AQP4.

Long Chen
Medical College of Shihezi University
Yu-qi Yang
Medical College of Shihezi University
Xue-rui Li
Medical College of Shihezi University
Zi-yi Feng
Medical College of Shihezi University
Zi-wei Han
No.951 General Hospital of xinjiang Military Region
Ke-tao Ma
Medical Collgeg of Shihezi University
Li Li (Lily7588@163.com)
Medical College of Shihezi University https://orcid.org/0000-0001-8591-0676
Jun-qiang Si (sijunqiang@shzu.edu.cn)
Medical College of Shihezi University

Research article

Keywords: presbyacusis; spiral ganglion neuron ; estrogen; aquaporin-4; apoptosis

Posted Date: April 28th, 2020

DOI: https://doi.org/10.21203/rs.3.rs-24016/v1

Abstract

Background

Estrogen has a protective effect on age-related hearing loss (ARHL), but the mechanism has not been elucidated. Cochlear spiral ganglion neurons (SGN) are an important link between the cochlear hair cells and the auditory center. This study used C57BL/6J mice as models of elderly individuals to observe the protective effect of estrogen against cochlear spiral ganglion cell apoptosis.

Methods

Fifty mice were divided into the following five groups (10 mice/group): the young group at 3 months of age (3 m), the elderly group at 12 months of age (12 m), the ovariectomized group at 12 months of age (12 m ovx), the ovariectomized group at 12 months of age + estrogen treatment for 1 month (E2 1 m), and the ovariectomized group at 12 months of age + estrogen treatment for 2 months (E2 2 m). The auditory brain stem response (ABR) was analyzed to detect changes in the hearing threshold, enzyme-linked immunosorbent assays (ELISAs) were used to determine the serum estrogen levels,Hematoxylin eosin (HE) staining and transmission electron microscopy (TEM) were used to observe the morphological changes in the cochlea spiral ganglion neurons (SGN), and TUNEL staining was used to observe the apoptosis of SGN. The expression of AQP4 was observed by immunofluorescence, and the mRNA expression levels of AQP4, Caspase-3, Bax and Bcl-2 in the cochlea spiral ganglion were determined by qRT-PCR. Cell experiments: Primary cultures of spiral ganglion cells were divided into a control group (SGC), DMSO group, D-gal group, D-gal + E2 group, D-gal + TGN020 group and D-gal + E2 + TGN020 group. Immunofluorescence was used to observe the AQP4 expression, qRT-PCR was used to observe the AQP4, Caspase-3, Bax and Bcl-2 mRNA expression levels, and flow cytometry was used to observe the apoptosis rate.

Results

An increased hearing threshold was observed in the elderly mice ($P < 0.001$). After removal of the ovaries, the hearing threshold of the mice in the 12 m ovx group was higher than it was in the 12 m control group ($P < 0.05$), and this increased threshold was accompanied by an increased loss of spiral ganglion cells, increased apoptosis ($P < 0.01$), and increased AQP4 expression ($P < 0.001$). Treatment with exogenous estrogen reversed all these changes. Cell experiments: D-gal increased the apoptosis rate ($P < 0.001$) and AQP4 expression ($P < 0.001$). Estrogen and the AQP4 inhibitor TGN020 both reduced the apoptosis rate and AQP4 expression.

Conclusion

Estrogen inhibited apoptosis of cochlear spiral ganglion cells in aged C57BL/6J mice by downregulating AQP4, thus achieving a protective effect on ARHL.

Background

Presbycusis, also known as age-related hearing loss (ARHL), is the most common sensory dysfunction in the elderly population (Nienke C Homans et al., 2016). While ARHL seriously affects the quality of life of elderly people, it also threatens the physical and psychological health of this population (Ciorba A et al., 2015). Neurogenic ARHL is a kind of deafness characterized by progressive degeneration of spiral ganglion neurons in the cochlea and high-frequency hearing loss. Neurogenic ARHL is the most common form of deafness in the elderly population (Mcfadden Sl et al., 1999; Bao J et al., 2010). Spiral ganglion neurons are an important junction between cochlear hair cells and the auditory center. Therefore, the age-related degeneration of SGN in the peripheral nervous system is the main reason for the occurrence and development of ARHL (Tang X et al., 2014).

Aquaporins (AQPs) are a family of membrane proteins that can transport water molecules (Ishibashi K et al., 2009). The imbalance of water homeostasis in the inner ear is closely related to inner ear disease, and AQP4 is widely distributed in the inner ear. Studies have shown that AQP4 can maintain endolymphatic homeostasis by regulating cellular osmotic pressure and K^+ concentrations (Li J et al.,2001). In addition, mice with AQP4 knocked out showed varying degrees of hearing loss (Eckhard A et al., 2012). Nathan Christensen et al. found that the content of AQP4 in the cochlea of CBA mice gradually decreased with age, and a study suggested that hearing loss may be related to the expression of AQP4 (Christensen N et al., 2009). These results suggest that the expression of AQP4 is closely related to hearing.

Estrogen is a steroid sex hormone, and studies have shown that it has a protective effect on hearing (Hill Ra et al., 2009). Studies have shown that the hearing threshold of women continues to decline after menopause, and the most significant decline occurs in the two years before and after menopause (K. Charitidi et al., 2010). Exogenous estrogen can reduce hearing loss in perimenopausal women (Zárate S et al., 2017). These results indicate that estrogen has a protective effect on ARHL, but how to exploit its protective effect is not yet clear. Estrogen can reduce nerve injury in the cerebral cortex of rats by regulating AQP4 (Shin Ja et al., 2011), and SGN apoptosis is an important reason for ARHL. Whether estrogen can inhibit the apoptosis of cochlear SGN by regulating AQP4 has not been reported.

In this study, C57BL/6 female mice were used as a model of ARHL. We performed ovarian removal and exogenous estrogen administration to observe the effect of estrogen on SGN cell apoptosis during ARHL. We used D-gal to treat primary cultured spiral ganglion cells (SGCs) to establish a model of aging to further explore the protective effect of estrogen on ARHL at the cellular level.

Methods

Animal preparation and experimental groups

C57BL/6J female mice (25-35 g) without ear disease were provided by the Beijing Weitonglihua Animal Center. The 50 mice were randomly divided into groups. The young group included 3-month-old mice (3 m, n=10). The elderly group included 12-month-old mice that were randomly assigned to the following

four subgroups (n = 10 for each group): (1) the sham group (12 m); (2) the ovx group that underwent bilateral ovariectomy at the age of 9 months (12 m ovx); (3) the 12 months ovariectomy +1 month estrogen treatment group that underwent bilateral ovariectomy at the age of 9 months and, after 8 weeks, received estrogen (100 μg/kg/day) (Fabiola Olivieri et al., 2014) subcutaneously for 4 weeks until 12 months of age (E2 1 m); and (4) the 12 months ovariectomy +2 months estrogen treatment group that underwent bilateral ovariectomy at the age of 9 months, and after 4 weeks, received estrogen (100 μg/kg/day) subcutaneously for 8 weeks until 12 months of age (E2 2m). All the experimental procedures were performed in accordance with the National Institutes of Health Guide for the Care and Use of Laboratory Animals (NIH Publications No. 80-23, revised 1996) and approved by the Committee of Animal Experimental Ethics of The First Affiliated Hospital of Medical College, Shihezi University (Shihezi, China) (No. A2018-160-01).

Auditory brainstem response (ABR) threshold test

The mice were anesthetized by intraperitoneal injection of 2% sodium pentobarbital and then placed in a sound screen room. A recording electrode was placed subcutaneously in the middle of the skull, a reference electrode was placed in the bilateral mastoid process, and a grounding electrode was placed at the tip of the nose. Both sides were given short acoustic stimuli with an intensity of 10~90 dB nHL and an interval of 20 db nHL. The scanning time was 10 s, the superposition was 1024 times, the stimulus interval was 11.10 times/s, and the V wave was used as the standard to determine the response threshold.

Measurement of estrogen levels by enzyme-linked immunosorbent assay (ELISA)

Blood samples were taken from each group and coagulated in warm water for approximately 15 min. The samples were centrifuged for 20 min to separate and collect the serum, and then, the estrogen levels were measured following the instructions of the estrogen detection kit (Clone Cloud, Wuhan China).

Cochlear histology

The mice were anesthetized with 2% sodium pentobarbital, and then, a thoracotomy was performed. The mice were perfused with saline and 4% paraformaldehyde (PFA) for fixation; then, the mouse necks were broken, and the bilateral cochlea were rapidly removed. The cochlea was fixed with 4% PFA and incubated for 24 h at 4 °C. Then, paraffin embedding was performed after decalcification with 10% ethylenediaminetetraacetic acid (EDTA) for 1 week. Continuous sections were cut parallel to the cochlear axis with thicknesses of 4 μm. Then, the sections were stained with hematoxylin and eosin (HE) and observed under a microscope (Olympus BX71, Japan).

Terminal deoxynucleotidyl transferase dUTP nick-end labeling (TUNEL) staining

After dewaxing the paraffin sections, they were boiled in citrate solution for 15 min. For analysis with an in situ cell death assay kit (Roche Holding, Basel, Switzerland), the cochlear sections were incubated in the dark with a mixture of labeled nucleotides and terminal nucleotide transferases (37°C, 1 h). The

sections were then observed with a Olympus laser confocal microscope (Zeiss LSM 510 META, Carl Zeiss AG), and the images were analyzed by Image-pro Plus 6.0 software.

Transmission electron microscopy (TEM)

The cochlea was exposed to 2.5% glutaraldehyde overnight at 4°C. The cells were decalcified in 10% EDTA for 1 week and fixed in 1% osmium tetroxide at room temperature for 2 h. The samples were immersed in an acetone/epoxy 618 mixture and then embedded in epoxy 618. The embedded material was sliced into ultrathin sections (50 nm) and then stained with uranium acetate and lead copper citrate. The ultrastructure of the stained sections was observed by transmission electron microscopy (FEI Tecnai G2 spirit, USA).

Immunofluorescence

The paraffin sections were dewaxed and boiled in a citrate solution (Sigma-Aldrich) to repair the antigens. The sections were permeabilized in 1% Triton-X100 and sealed with a 5% BSA (Sigma-Aldrich) solution for 1 h. The primary antibodies were diluted with a 5% BSA solution, and the sections were incubated with these antibodies at 4°C for 12 h. The antibodies included rabbit anti-AQP4 (1:200 Abcam, ab46182) and mouse anti-TUJ1 (1:200, Abcam, ab78078). After washing with PBS (Sigma-Aldrich, USA) three times, the sections were incubated with the secondary antibodies (diluted with 5% BSA solution) at room temperature without light for 1 h. The secondary antibodies included goat anti-rabbit or anti-mouse secondary antibodies (1:100; Beijing Fir Jinqiao Biotechnology Co. Beijing, China). After staining with 4,6-diamino-2-phenyl indole (DAPI; Solarbio), the sections were sealed with an anti-fluorescence quenching agent, and the fluorescence intensity was observed by the LCSM method. The average fluorescence intensity (MFI) was used to present the protein expression level.

Quantitative real-time polymerase chain reaction (qRT-PCR)

The cochlea was extracted from the mice in each group under aseptic conditions, and the volute, basement membrane, spiral ligament, and central axis were removed. The reverse transcription of RNA into complementary DNA (cDNA) was performed via an AMV First-Strand cDNA synthesis kit (Solarbio Life Science, Beijing, China) with 20 mg of tissues (the cells were cultured from 10^7 spiral ganglion cells) according to the manufacturer's directions. qRT-PCR was performed via LightCycler 480 Software (Thermo Fisher Scientific, Waltham, MA, USA) with Power SYBR Green (Thermo Fisher Scientific, Waltham, MA, USA) The conditions for the reverse transcription were predenaturation at 70°C for 5 min, annealing at 42°C for 60 min, and extension at 4°C for 5 min. The primers used for the amplification of the target genes and the internal standards were as follows:

B-actin: 5'- ACTGCTCTGGCTCCTAGCAC -3'

3'- ACATCTGCTGGAAGGTGGAC -5';

AQP4: 5'- CTCATCTCCCTCTGCTTTGG-3'

3'- CGATGCTGATCTTTCGTGTG -5';

Caspase 3: 5'- TGGTGATGAAGGGGTCATTTATG -3'

3'- TTCGGCTTTCCAGTCAGACTC -5';

Bax: 5'- TGAAGACAGGGGCCTTTTTG -3'

3'- AATTCGCCGGAGACACTCG -5';

Bcl-2: 5'- ACGGTGGTGGAGGAACTCTTCAG-3'

3'- GGTGTGCAGATGCCGGTTCAG -5'.

The reaction conditions of the qRT-PCR were as follows: predenaturation at 95°C for 2 min, denaturation at 95°C for 5 s, and annealing at 60°C for 10 s, and this cycle was repeated 40 times.

SGC primary culture and identification

Newborn C57BL/6J suckling mice (0-3 days old) were selected, and 75% alcohol immersion disinfection was performed for 3~5 min. Anesthesia was followed by decapitation, and then the bilateral temporal bone was separated and immersed in prechilled D-Hanks solution (containing 100 U/ml penicillin +100 U/ml streptomycin) at 4°C. The auditory vesicles were fully exposed under an anatomical microscope. The membranous labyrinth, helical ligament and stripped basement membrane were removed. The tissue of the cochlear axis spiral tube containing the spiral ganglion neurons was rapidly transferred into a 1-ml centrifuge tube containing 0.125% type collagenase and 0.125% trypsin. The centrifuge tube was incubated in a 37°C incubator for 20 min, and cell culture medium (90% DMEM/F12 (No. C11330500, Gibco, Thermo Fisher Scientific, China)+10% FBS (No. 04-001-A; Biological Industries, Cornwell, CT, USA)+100 u/ml penicillin + streptomycin) was added to stop the digestion. The cell suspension was centrifuged, and the supernatant was discarded. The cell culture medium was added to resuspend the SGCs. Cell counts were performed under an optical microscope, and the cells were plated at a density of 1×10^6 cells/ml on a cover glass or 6-well plates precoated with 0.05% polylysine. The culture medium was changed to B-27 (Gibco, Grand Island, NY, USA) neural base medium (90% DMEM/F12+10% b-27+100 u/ml penicillin + streptomycin) after the cells attached to the well. Approximately 50% of the medium was changed every 3 days. After 7 days, the neurons were treated with D-gal (V900922-100G; Sigma-Aldrich), which was dissolved in serum-free 10% B-27-supplemented neurobasal medium. The cells were cultured for 7 days, and 50% of the medium was changed every 3 days during this period. The medium was replaced after adding the AQP4 inhibitor TGN020 (100 nM) (Olivieri F et al., 2014) (Sigma-Aldrich, SML0136, St. Louis, MO, USA) to the pretreated neurons with D-gal. Estrogen (10 nM) (Wu Sy et al., 2016) (Duenas M et al., 1996) was added to the cells in petri dishes and incubated for 24 h. All the neuron cells were cultured in an incubator with 5% carbon dioxide at 37°C.

Cell identification: After the primary SGCs were cultured, the medium was removed from the petri dish, and 4% paraformaldehyde was added for fixation. The cells were permeabilized with 0.3% Triton X-100 for 15 min and then blocked with 5% BSA. The primary antibody against the TUJ-1 protein (1:100) was added, and the cells were placed in a wet box and incubated at 4°C overnight. The cells were then incubated with a FITC-conjugated secondary antibody (1:100) for 1 h at room temperature in the dark. The nuclei were stained with DAPI, and an anti-fluorescence quenching agent was added. Then, the cells were examined under a fluorescence microscope to collect the images.

Cell viability and cell senescence tests

The cells were cultured in a 96-well microwell plate for 7 days, and D-gal was added at different concentrations for 7 days of intervention. The cell viability was then measured by the cell counting kit-8 (CCK-8, Dojindo Laboratories, Kumamoto, Japan). The cellular senescence was evaluated by means of a β-galactosidase staining kit (No. C0602; Beyotime Biotechnology, Haimen, China).

Flow cytometry

An Annexin V-FITC/PI double-staining apoptosis kit was used to detect the apoptosis of cultured neurons. The cells were rinsed twice with cold PBS and incubated with EDTA-free 0.25% trypsin at 37°C until 80% of the cells were detached. The cell suspensions were collected, centrifuged at 1000 rpm for 5 min. Then, the supernatant was discarded, and the cells were washed twice with PBS. The cells were resuspended in 500 μl of 1× binding buffer containing 10 μl of annexin V-FITC and 5 μl PI. The cells were incubated at room temperature in the dark for 15 min and then analyzed by flow cytometry.

Statistical analysis

SPSS 19.0 software was used for the statistical analyses, and GraphPad Prism 6.01 software was used to generate the graphs. All the data are expressed as the means ± standard deviations. One-way ANOVA was used for comparisons between groups, LSD-t tests were used for pairwise comparisons between groups, multivariate analysis of variance was used to compare multiple groups at different time points. A p-value of less than 0.05 was considered to be statistically significant.

Results

Effects of estrogen on hearing in mice (Fig. 1)

Estrogen levels in the mice in each group

Figure 1A shows a schematic diagram of estrogen administration. The ELISA results showed that there was no significant difference in the estrogen levels between the 3 m group and the 12 m group. Compared with those in the 12 m group, the estrogen levels in the 12 m ovx group decreased significantly ($P<0.001$). Compared with those in the 12 m ovx group, the estrogen levels in the E2 1 m and E2 2 m groups were significantly increased ($P<0.001$). (Figure 1B).

ABR detected changes in the hearing threshold in each group

The auditory brain stem response (ABR) was used to assess the hearing of the C57BL/6 J mice. Within an interval of 10 dB nHL, the sound stimulus intensity gradually decreased from 90 dB nHL to 10 dB nHL, and then, we recorded the changes in the V waves in the acoustic stimulus threshold of each group. The results showed that the ABR threshold increased with age, and compared with that of the 3 m group, the threshold of the 12 m group was significantly increased ($P<0.001$). After ovariectomy, the threshold decreased compared with that of normal mice. Compared with that in the 12 m group, the threshold in the 12 m OVX group was increased ($P<0.05$). After estrogen injection, the thresholds of the E2 1 m group and the E2 2 m group were significantly lower than those of the 12 m OVX group ($P<0.05$) (Figure 1C).

Protective effect of estrogen on spiral ganglion neurons in mouse cochlea (Fig. 2)

Histopathological changes of the cochlea SGN

The left cochlea was harvested from each group, and the histopathological changes in the SGN were observed by HE staining. As shown in Figure 2A, the SGN structure in the 3 m group was clear, the abundant nerve cells were regularly arranged, and the ratio of nuclear pulp was normal (Figure 2Aa). The number of nerve cells in the 12 m group decreased, and the ratio of the nuclear pulp was altered (Figure 2Ab). The SGN cells in the 12 m ovx group were loose in structure, irregular in shape and disordered in arrangement, nuclear condensation, and chromatin edging(Figure 2Ac). In contrast, the E2 1 m group (Figure 2Ad) and E2 2 m group (Figure 2Ae) exhibited different degrees of reduced nerve cell injury, and the number of injured nerve cells with relatively complete cell structure was reduced.

Cochlea SGN injury in each group

The SGN ultrastructure was observed by transmission electron microscopy to evaluate neuronal damage (Figure 2B). The results showed that in the 3 m group, the cell structure was basically intact, the cytoplasm was slightly dissolved, the mitochondrial arrangement was orderly, and the chromatin was basically normal (Figure 2Ba). In the 12 m group, the cytoplasmic vacuoles were obvious, the mitochondrial cristae were dissolved, and the euchromatin was dissolved in the nucleus (Figure 2Bb). In the 12 m ovx group, the cytoplasm was obviously vacuolized, the numbers of mitochondria were reduced, the nuclear membrane was pitted and dissoluted, and the euchromatin and heterochromatin were absent (Figure 2Bc). In the E2 1 m group, cytoplasmic vacuoles, mitochondrial cristolysis, organelle depletion, nuclear chromatin dissolution, and a relatively intact nuclear membrane were observed (Figure 2Bd). In the E2 2 m group, cytoplasmic vacuoles were formed, mitochondrial cristae were dissolved, euchromatin was absent in the nucleus, and the nuclear membrane was complete (Figure 2Be).

Injury to SGN neurons in the cochlea and apoptosis in each group

TUNEL staining was used to observe the apoptosis of the helical ganglion cells in each group. Apoptosis was more serious in the 12 m group than in the 3 m group, and apoptosis was increased in the 12 m ovx group compared with the 12 m group ($P<0.001$). The degree of apoptosis in the E2 1 m group was

decreased after estrogen administration compared with that in the 12 m ovx group (P<0.001). Compared with that of the 12 m ovx group, the apoptosis of the E2 2 m group was significantly reduced (P<0.001), and the apoptosis of the E2 1 m group was significantly improved (P<0.001) (Figure 2C).

Estrogen downregulated AQP4 and apoptotic proteins (Fig. 3)

Effect of estrogen on AQP4 expression

The expression of AQP4 in the helical ganglia was observed by immunofluorescence. As shown in Figure 5A, AQP4 was labeled with green fluorescence, and TUJ1 was labeled with red fluorescence. As shown in Figure 5B, the semiquantitative statistical analysis of AQP4 indicated that compared with that in the 12 m group, AQP4 expression was enhanced in the 12 m ovx group (P<0.001). In addition, AQP4 expression decreased in the E2 1 m group and E2 2 m group (P<0.001) (Figure 3A).

Expression of AQP4, Caspase3, Bax and bcl-2 mRNA in each group

qRT-PCR was used to detect the mRNA levels of Bcl-2 in the spiral ganglion. Compared to those in the 3 m group, the mRNA levels of the apoptotic proteins Caspase3 and Bax in the 12 m group were increased (P<0.05), and the mRNA level of the anti-apoptotic protein Bcl-2 was significantly decreased (P<0.01). Compared with those in the 12 m group, the mRNA levels of AQP4, Caspase3 and Bax were significantly increased, while the level of Bcl-2 was increased, in the 12 m ovx group (P<0.01). Compared with that in the 12 m ovx group, the apoptotic protein caspase-3 mRNA level was decreased (P<0.01), the Bax level was decreased (P<0.001), and the anti-apoptotic protein Bcl-2 mRNA level was increased (P<0.05). Compared with those of the 12 m ovx group, the caspase-3 and Bax mRNA levels of the E2 2 m group were decreased (P<0.01), and the mRNA level of the anti-apoptotic protein Bcl-2 was increased (P<0.01). All the above data are statistically significant (Figure 3B, Figure 3C).

SGC primary culture and senescence model preparation (Fig. 4)

SGC primary culture and identification

Primary spiral ganglion cells were cultured and purified (Figure 4A). The spiral ganglionic cells were identified with the nerve cell marker TUJ1 (green fluorescence), and prokaryotes were labeled with DAPI (blue fluorescence) (Figure 4B).

D-gal treatment of SGCs to establish a senescence model

D-gal decreased neuronal activity in a dose-dependent manner. The results were statistically significant at a concentration of 10 mg/ml (P < 0.05, Figure 4E). When the concentration of D-gal was greater than 15 mg/ml, the cellular activity was significantly decreased, and the D-gal staining results are shown in Figure 4C. In addition, the number of positive cells decreased (P<0.001, Figure 4D). These results suggested that we successfully established a senescent cell model, and thus, we chose 10 mg/ml D-gal to induce neuronal senescence in the subsequent experiments.

Estrogen downregulated AQP4 expression and SGCs apoptosis (Fig. 5)

Effect of estrogen on AQP4 expression in SGCs

Immunofluorescence was used to observe the expression of AQP4 in each group. AQP4 was labeled green, TUJ1 nerve cells were labeled red, and DAPI nuclei were labeled blue. The AQP4 expression increased after D-gal treatment (P<0.001). After E2 was administered, the AQP4 expression in the D-gal+E2group was decreased in the D-gal group (P<0.001). In addition, the results showed that there was no significant difference in AQP4 expression between the DMSO group and SGC group (Figure 5A).

Apoptosis of SGCs in each group

Cell apoptosis was detected by flow cytometry, and the results showed that there was no significant difference in the apoptosis rate between the DMSO group and SGC group. After D-gal treatment, the number of apoptotic cells was increased (P<0,001). Compared with the D-gal group, the D-gal+E2 group showed decreased apoptosis (P<0,001). The D-gal+TGN020 group showed decreased apoptosis compared with the D-gal group (P<0,001). Compared with the D-gal group, the D-gal+E2+TGN020group showed decreased apoptosis (P<0,001) (Figure 5B).

Expression of AQP4, Caspase3, Bax and bcl-2 mRNA in SGCs of each group

The mRNA levels of AQP4 and the apoptotic proteins Caspase3, Bax, and Bcl-2 in each group were determined by qRT-PCR. The results showed that there was no significant difference in the mRNA levels between the DMSO group and the SGC group. Compared with those in the SGC group, the mRNA level of AQP4 was increased (P<0.05), the mRNA level of the apoptotic proteins Caspase3 and Bax were increased (P<0.001), and the mRNA level of the anti-apoptotic protein Bcl-2 was decreased (P<0.001) in the D-gal group. Compared with those in the D-gal group, the mRNA level of AQP4 was decreased (P<0.05), the mRNA levels of Caspase3 and Bax were decreased (P<0.01), and the mRNA level of Bcl-2 was increased (P<0.001) in the D-gal+E2group. Compared with those in the D-gal group, the mRNA level of AQP4 was reduced (P<0.001), the mRNA levels of Caspase3 and Bax were reduced (P<0.05), and the mRNA level of Bcl-2 was increased (P<0.01) in the D-gal+TGN020 group. Compared with those in the D-gal group, the mRNA level of AQP4 was reduced (P<0.001), the mRNA levels of Caspase3 and Bax were decreased (P<0.001), and the mRNA level of Bcl-2 was increased (P<0.001) in the D-gal+E2+TGN020group (Figure 5C, Figure 5D).

Discussion

ARHL is a common sensory dysfunction in the elderly population. It has been reported that estrogen has a certain protective effect on ARHL, but ways by which to exploit this effect remain unclear. In this experiment, C57BL/6J mice were selected to establish a model of ARHL. By observing the changes in spiral ganglion cellular apoptosis and AQP4 expression in the elderly mice, as well as the effect of

estrogen on this change, the protective effect of estrogen against ARHL, which is achieved by regulating AQP4 to inhibit spiral ganglion cell apoptosis, was observed.

C57BL/6J mice are inbred mice with Cdh23 gene mutations, are characterized by progressive hearing loss and precocious puberty, and are the most commonly used model mice for ARHL research (Keithley Em et al., 2004; Someya S et al., 2010). In this experiment, 3-month-old mice were included in the young group, and 12-month-old mice were included in the elderly group. The ABR test showed that the hearing threshold of the 12-month-old mice was significantly increased. Some studies have reported that in normal rats, ovariectomy leads to an increase in the ABR threshold, and estrogen replacement can reverse these changes (Coleman Jr et al., 1994). Moreover, estrogen replacement therapy can improve the amplitude and latency of DPOAEs and ABR in mice (Williamson Tt et al., 2019). In our study, after ovariectomy, the in vivo estrogen level was lower and the ABR threshold was higher than it was in normal elderly female mice; however, after exogenous estrogen administration, the in vivo estrogen level was maintained within the normal range, and the ABR threshold was lower than that of the ovariectomized mice. The results are consistent with the experiments mentioned above, suggesting that stable in vivo estrogen levels have a certain protective effect against hearing loss in elderly mice. Sensorineural ARHL is the most common type of ARHL, and it is mainly characterized by the gradual degeneration of cochlear hair cells and spiral ganglion neurons. The necrosis or apoptosis of spiral ganglion cells is one of the important mechanisms of ARHL (Sang L et al., 2017). At present, studies have preliminarily shown that the protective effect of estrogen against hearing loss may be related to the survival of neurons. Estrogen may play a protective role in nerve cells by regulating neurotrophic factors (Coleman Jr et al., 1994) and inhibiting apoptosis (Hill Ra et al., 2004; Bean La et al., 2015). In this experiment, histopathological changes in the spiral ganglion of the cochlea and ultrastructural neuronal damage were observed by HE staining and transmission electron microscopy. The results showed that the spiral ganglion of elderly C57BL/6J mice was obviously missing and that the neurons were damaged. After ovariectomy, the damage to the spiral ganglion in these mice was exacerbated. After estrogen was administered, the loss of the spiral ganglion and the degree of neuronal damage were significantly improved. The results suggest that estrogen can reduce the loss of the spiral ganglion and improve damage to neurons during ARHL. In the auditory system, damage to the spiral ganglion and hair cells is irreversible, which leads to permanent sensorineural deafness. At present, there is no effective drug for the prevention or treatment of ARHL, and hearing can only be improved through sound reinforcement by hearing aids or through electrical stimulation by cochlear implants. Cochlear implants can effectively replace the mechanical sensory transduction function of the lost hair cells through direct electrical stimulation of the spiral ganglion, but these devices only work when sufficient spiral ganglion is retained (Roehm Pc et al., 2005). Therefore, the protection of the spiral ganglion is very important for the prevention and treatment of ARHL. Studies show that after ERβ is knocked out, the number of cells spiral ganglion cells in 12-month-old mice decreases, and stable estrogen levels may help to maintain the integrity of ERs. The estrogen ligand and ER can be mutually regulated (Hill Ra et al., 2004), thus delaying the degeneration of auditory neurons. This observation is consistent with our results.

Studies have found that activation the apoptosis pathway in the mouse cochlea increases with age, and the age-related absence of spiral ganglion cells may be related to apoptosis. However, the mechanism by which spiral ganglion cell apoptosis participates in the occurrence and development of ARHL is still unclear. Apoptosis is mainly mediated by the exogenous pathway, which is triggered by the death receptor, and the endogenous pathway, which is initiated by mitochondria- and endoplasmic reticulum-dependent pathways (Someya S et al., 2010). Estrogen is known to inhibit neuronal apoptosis and increase neuronal survival. We observed apoptosis of the spiral ganglion in the mouse cochlea by TUNEL staining. The apoptosis in the elderly mice was obvious. The ovariectomized mice exhibited more severe apoptosis than the normal elderly female mice. However, after estrogen was administered, the apoptosis decreased. In addition, we further confirmed apoptosis at the cellular level in cell model of aging. D-gal is widely used in experimental research to establish models that simulate aging (Cui X et al., 2006). Research shows that D-gal can induce aging in neuron cells (Hattori F et al., 2007; Arnér Es et al., 2009) and even lead to apoptosis (Zeng L et al., 2014) by promoting the generation of ROS in cells. We used D-gal to treat spiral ganglion cells to establish a model of aging, and flow cytometry was used to assess apoptosis. The results showed that the apoptosis rate increased after D-gal treatment but decreased after estrogen administration.

To further explore the apoptotic pathway in the spiral ganglion during ARHL, we used qRT-PCR to detect changes in the Caspase-3, Bax, and Bcl-2 mRNA levels related to the endogenous pathway of apoptosis. Caspase-3 is considered the final effector protein of apoptosis, and its expression and activation levels will cause cell apoptosis to enter an irreversible stage (Fujimura M et al., 1999). We observed that the levels of Caspase-3 and Bax mRNA in the spiral ganglion of elderly mice increased while the levels of the anti-apoptosis factor Bcl-2 decreased. These results indicated that the endogenous apoptosis pathway was involved in the loss of the spiral ganglion during cochlear aging. Moreover, in ovariectomized mice, the mRNA levels of the apoptosis proteins were significantly upregulated, and the mRNA levels of the anti-apoptosis proteins was significantly reduced. In the cell experiment, estrogen downregulated the increased mRNA levels of the apoptosis proteins caused by D-gal treatment. These results suggest that estrogen can inhibit the apoptosis of the spiral ganglion during aging.

In the aging cochlea, glutamate excitotoxicity may lead to apoptosis of the spiral ganglion, while estrogen has been proven to inhibit the neuronal damage and apoptosis induced by glutamate excitotoxicity in the central nervous system (Zhao L et al., 2004). In addition, estrogen can reduce gentamicin-induced HC apoptosis by inhibiting the JNK-mediated apoptosis pathway (Nakamagoe M et al., 2010). Estrogen can also inhibit ROS-induced cochlear HC apoptosis by upregulating anti-apoptosis factors. Among them these factors, E2 is known to upregulate Bcl-2 and Bcl-XL in neurons in the central nervous system (Garcia-Segura Lm et al., 1998; Christian, J et al., 1999), and the presence of ERE sequences in these genes suggests that they may be direct targets of ERs (Perillo B et al., 2000). In addition, estrogen can induce Bcl-2 expression by rapidly activating the PI3K/Akt signaling pathway (Yune Ty et al., 2008). These pathways may be potential targets for the estrogen-mediated inhibition of apoptosis in spiral ganglion cells.

AQP4 is one of the most important water-selective channel proteins in the central nervous system. AQP4 is widely distributed in the astrocytes and retinal optic ganglia in the brain (Previch Le et al., 2016), but its expression and function in the spiral ganglion of the cochlea have been rarely studied. The expression of AQP4 in the spiral ganglion of the cochlea of C57BL/6J mice was determined by immunofluorescence using an AQP4 antibody and the nerve cell marker TUJ1. We found that the expression of AQP4 in spiral ganglion cells of the ovariectomized mice was increased. After estrogen was administered, the expression of AQP4 was decreased. In the cell experiments, after D-gal treatment, the expression of AQP4 in the spiral ganglion cells was increased, and after estrogen was administered, the expression was decreased. It is suggested that estrogen can downregulate the expression of AQP4 in the spiral ganglion. Research shows that estrogen can upregulate AQP4 in the cerebral cortex of rats in a rat model of stroke (Szabo C et al., 2014), while estrogen can also downregulate AQP4 in the brain of rats in a model of traumatic brain injury to achieve protection of the brain (Charitidi K et al., 2010). Therefore, the evidence regarding the regulation of aquaporins by estrogen is contradictory, and the differences may depend on the type of injury. The regulation of AQP4 by estrogen can be inhibited by ICI182780, which is a common antagonist of the ERα or ERβ receptors, suggesting that estrogen may regulate AQP4 through ERs, and the activity of AQP4 can be regulated through the activation of protein kinase A, calcium/calmodulin dependent protein kinase and protein kinase C, which are also affected by estrogen (Menardo J et al., 2012).

In the cell experiment, we found that the apoptosis rate of the spiral ganglion cells increased after D-gal treatment, while the apoptosis rate decreased after the AQP4 inhibitor was added, and the qRT-PCR and flow cytometry results suggested reduced apoptosis. We speculated that the increased expression of AQP4 might lead to apoptosis of spiral ganglion cells. Inflammatory factors in the cochlea increase during aging (Zhao Cq et al., 2007). Inflammatory factors, such as IL-1β and TNF-α, can induce apoptotic cascade reactions, further activating Caspase-3 and promoting cell apoptosis (Cheng W et al., 2013). Other studies have shown that the downregulation of AQP4 can inhibit inflammatory factors and thus reduce nerve injury (Liu S et al., 2017). This mechanism may be a way for APQ4 to participate in the apoptosis of spiral ganglion cells. Glutamic acid accumulation in the cochlea can cause loss of organelle function and reduced expression of apoptosis factors, thus causing hearing loss (Wang Y et al., 2010). However, inhibiting the upregulation of AQP4 can reduce the excessive glutamate release caused by ischemia. We assume that changes in AQP4 may cause the accumulation of glutamate, thus affecting the apoptosis of spiral ganglion cells. In this experiment, estrogen downregulated the expression of AQP4 in the spiral ganglion. In a rat model of traumatic brain injury, the upregulation of AQP4 can aggravate neuronal apoptosis in the brain, while estrogen can reduce apoptosis by the downregulation of AQP4 (Charitidi K et al., 2010). Therefore, we suggest that estrogen may inhibit the apoptosis of spiral ganglion cells by downregulating AQP4 in the spiral ganglion cells. The specific interaction between AQP4 and apoptosis and the mechanism by which estrogen regulates AQP4 need further study.

Conclusion

In summary, this experiment found that estrogen deficiency can lead to increased apoptosis of spiral ganglion cells and decreased hearing in C57BL/6J mice during aging and that estrogen treatment can reverse these changes. In the D-gal-induced cell model of aging, estrogen downregulates the expression of AQP4 in the spiral ganglion of the cochlea, thus inhibiting cell apoptosis. The loss and apoptosis of spiral ganglion cells is an irreversible phenomenon. Our research proves that estrogen can inhibit the apoptosis of spiral ganglion cells in elderly mice by downregulating AQP4, thus exerting its protective effect on hearing. This study will provide a new experimental basis for estrogen-mediated hearing protection. However, the mechanism by which estrogen regulates AQP4 still needs further research.

Abbreviations

ARHL
age-related hearing loss
SGN
spiral ganglion neurons
ABR
auditory brain stem response
ELISA
senzyme-linked immunosorbent assays
TEM
transmission electron microscopy
TUNEL
TdT-mediated dUTP nick-end labeling
PBS
Phosphate buffered saline
BSA
Bull Serum Albumin
qRT-PCR
Quantitative real-time polymerase chain reaction

Declarations

Availability of data and materials

Data could be obtained upon request to the corresponding author.

Acknowledgments

We acknowledge and appreciate our classmates for their valuable efforts and comments on this paper.

Funding

This study was supported by the Natural Science Foundation of China (Grants 81560175、81960188). This study was performed at the Key Laboratory of Xinjiang Endemic and Ethnic Diseases in the Xinjiang Provincial Department of Physiology, School of Medicine, Shihezi University.

Author informatio

Affiliations

Department of Physiology, Medical College of Shihezi University, Shihezi, Xinjiang 832002, China

Long Chen ,Yu-qi Yang ,Xue-rui Li ,Zi-yi Feng , Ke-tao Ma ,Li Li,

Jun-qiang Si

Long Chen Email：chenllong314@163.com

Yu-qi Yang Email：441875209@qq.com

Xue-rui Li Email：lixuerui020@163.com

Zi-yi Feng Email：572840499@qq.com

Ke-tao Ma Email：maketao@hotmail.com

Li Li Email： Lily7588@163.com

Jun-qiang Si Email：sijunqiang@shzu.edu.cn

Department of Physiology, Medical College of Jiaxing, Jiaxing, Zhejiang 3410000

Li Li Email： Lily7588@163.com

No. 951 General Hospital of Xinjiang Military Region, Kuerle 841000 China

Zi-we Han Email：455934298@qq.com

Contributions

Long Chen conceived and designed the study.Long Chen and Yu-qi Yang performed the experiments. Xue-rui Li ,Zi-yi Feng and Zi-we Han Assist in the experiment. Long Chen analyzed the data and fnished the essay.Li Li and Jun-qiang Si contributed to revising the manuscript. Ke-tao Ma coordinated and directed the project. All authors read and approved the fnal manuscript.

Corresponding author

Correspondence to Li Li and Junqiang Si

Li Li Email Lily7588@163.com

Jun-qiang Si Email sijunqiang@shzu.edu.cn

Ethics declarations

Ethics approval and consent to participate

The protocol was approved by the Animal Care and Use Committee of the First Afliated Hospital of the Medical College at Shihezi University(No. A2018-160-01) and was conducted in strict accordance with the guidelines of the Guide for the Care and Use of Laboratory mice.

Consent for publication

Consent for publication was obtained from the participants.

Competing interests

The authors declare that there are no competing interest.

References

Ciorba A, S, Hatzopoulos, C, Bianchini, C, Aimoni, H, Skarzynski, immunopathology, Skarzynski PH et al. %J International journal of.(2015). Genetics of presbycusis and presbystasis. *28*(1), 29-35. doi:10.1177/0394632015570819

Eckhard A, C, Gleiser, H, Arnold, H, Rask-Andersen, H, Kumagami, M, Müller, et al. (2012). Water channel proteins in the inner ear and their link to hearing impairment and deafness. *33*, 612-637. doi:10.1016/j.mam.2012.06.004

Elias S.J. Arnér %J Bba General Subjects. (2009). Focus on mammalian thioredoxin reductases–important selenoproteins with versatile functions. *1790*(6), 495-526. doi:10.1016/j.bbagen.2009.01.014

Perillo B, A, Sasso, C, Abbondanza, Molecular, Palumbo G %J Cellular Biology, . (2000). 17beta-estradiol inhibits apoptosis in MCF-7 cells, inducing bcl-2 expression via two estrogen-responsive elements present in the coding sequence. *20*(8), 2890-2901. doi:10.1128/mcb.20.8.2890-2901.2000

Szabo C, C, Ransy, K, Módis, M, Andriamihaja, B, Murghes, C, Coletta, et al. (2014). Regulation of mitochondrial bioenergetic function by hydrogen sulfide. Part I. Biochemical and physiological mechanisms. *171*(8), 2099-2122. doi:10.1111/bph.12369

K. Charitidi, Frisina, R D, Vasilyeva, O N, Zhu, X., & Canlon, B. %J Neuroscience. (2010). Expression patterns of estrogen receptors in the central auditory system change in prepubertal and aged mice. *170*(4), 1270-1281.

Zhao CQ, D, Liu, H, Li, LS, Jiang, & Dai LY %J Apoptosis : an international journal on programmed cell death. (2007). Interleukin-1beta enhances the effect of serum deprivation on rat annular cell apoptosis. *12*(12), 2155-2161. doi:10.1007/s10495-007-0137-x

Keithley EM, C, Canto, QY, Zheng, N, Fischel-Ghodsian, & Johnson KR %J Hearing research. (2004). Age-related hearing loss and the ahl locus in mice. *188*, 21-28. doi:10.1016/s0378-5955(03)00365-4

Hattori F, & Oikawa S %J Sub-cellular Biochemistry,. (2007). Peroxiredoxins in the central nervous system. *44*, 357-374. doi:10.1007/978-1-4020-6051-9_17

Olivieri F, M, Ahtiainen, R, Lazzarini, E, Pöllänen, M, Capri, M, Lorenzi, et al. (2014). Hormone replacement therapy enhances IGF-1 signaling in skeletal muscle by diminishing miR-182 and miR-223 expressions: a study on postmenopausal monozygotic twin pairs. *13*(5), 850-861. doi:10.1111/acel.12245

Nienke C Homans, Metselaar, R Mick, Dingemanse, J Gertjan, Schroeff, Marc P Van Der, & Goedegebure, André %J Laryngoscope. (2016). Prevalence of age-related hearing loss, including sex differences, in older adults in a large cohort study. *127*(3), 725-730.

Bao J, & Ohlemiller KK %J Hearing research. (2010). Age-related loss of spiral ganglion neurons. *264*, 93-97. doi:10.1016/j.heares.2009.10.009

Li J, & chemistry, Verkman AS %J The Journal of biological. (2001). Impaired hearing in mice lacking aquaporin-4 water channels. *276*(33), 31233-31237. doi:10.1074/jbc.M104368200

Menardo J, Y, Tang, S, Ladrech, M, Lenoir, F, Casas, C, Michel, et al. (2012). Oxidative stress, inflammation, and autophagic stress as the key mechanisms of premature age-related hearing loss in SAMP8 mouse Cochlea. *16*(3), 263-274. doi:10.1089/ars.2011.4037

Shin JA, JH, Choi, YH, Choi, & acta, Park EM %J Biochimica et biophysica. (2011). Conserved aquaporin 4 levels associated with reduction of brain edema are mediated by estrogen in the ischemic brain after experimental stroke. *1812*(9), 1154-1163. doi:10.1016/j.bbadis.2011.05.004

Coleman JR, D, Campbell, WA, Cooper, MG, Welsh, & Moyer J %J Hearing research. (1994). Auditory brainstem responses after ovariectomy and estrogen replacement in rat. *80*(2), 209-215. doi:10.1016/0378-5955(94)90112-0

Charitidi K, RD, Frisina, ON, Vasilyeva, X, Zhu, & Canlon B %J Neuroscience. (2010). Expression patterns of estrogen receptors in the central auditory system change in prepubertal and aged mice. *170*(4), 1270-1281. doi:10.1016/j.neuroscience.2010.08.010

Ishibashi K, S, Hara, Clinical, & Kondo S %J,Experimental Nephrology. (2009). Aquaporin water channels in mammals. *13*(2), 107-117. doi:10.1007/s10157-008-0118-6

Sang L, T, Zheng, L, Min, X, Zhang, X, Ma, S, Entenman, et al. (2017). Otoprotective effects of ethosuximide in NOD/LtJ mice with age-related hearing loss. *40*(1), 146-154. doi:10.3892/ijmm.2017.3004

Zeng L, Y, Yang, Y, Hu, Y, Sun, Z, Du, Z, Xie, et al. (2014). Age-related decrease in the mitochondrial sirtuin deacetylase Sirt3 expression associated with ROS accumulation in the auditory cortex of the mimetic aging rat model. *9*(2), e88019. doi:10.1371/journal.pone.0088019

Zhao L, TW, Wu, & Brinton RD %J Brain Research. (2004). Estrogen receptor subtypes alpha and beta contribute to neuroprotection and increased Bcl-2 expression in primary hippocampal neurons. *1010*, 22-34. doi:10.1016/j.brainres.2004.02.066

Bean LA, A, Kumar, A, Rani, M, Guidi, AM, Rosario, PE, Cruz, et al. (2015). Re-Opening the Critical Window for Estrogen Therapy. *35*(49), 16077-16093. doi:10.1523/jneurosci.1890-15.2015

Previch LE, L, Ma, JC, Wright, S, Singh, X, Geng, & sciences, Ding Y %J International Journal of Molecular. (2016). Progress in AQP Research and New Developments in Therapeutic Approaches to Ischemic and Hemorrhagic Stroke. *17*(7). doi:10.3390/ijms17071146

Garcia-Segura LM, P, Cardona-Gomez, F, Naftolin, &Chowen JA %J Neuroreport. (1998). Estradiol upregulates Bcl-2 expression in adult brain neurons. *9*(4), 593-597. doi:10.1097/00001756-199803090-00006

Duenas M, I, Torres-Aleman, F, Naftolin, & Garcia-Segura LM %J Neuroscience. (1996). Interaction of insulin-like growth factor-I and estradiol signaling pathways on hypothalamic neuronal differentiation. *74*(2), 531-539. doi:10.1016/0306-4522(96)00142-x

Fujimura M, Y, Morita-Fujimura, M, Kawase, JC, Copin, B, Calagui, CJ, Epstein, et al. (1999). Manganese superoxide dismutase mediates the early release of mitochondrial cytochrome C and subsequent DNA fragmentation after permanent focal cerebral ischemia in mice. *19*(9), 3414-3422. doi:10.1523/jneurosci.19-09-03414.1999

Nakamagoe M, K, Tabuchi, I, Uemaetomari, B, Nishimura, & Hara A %J Hearing research. (2010). Estradiol protects the cochlea against gentamicin ototoxicity through inhibition of the JNK pathway. *261*, 67-74. doi:10.1016/j.heares.2010.01.004

Christensen N, M, D'Souza, X, Zhu, & Frisina RD %J Brain Research. (2009). Age-related hearing loss: aquaporin 4 gene expression changes in the mouse cochlea and auditory midbrain. *1253*, 27-34. doi:10.1016/j.brainres.2008.11.070

Pike CJ %J Journal of Neurochemistry. (1999). Estrogen modulates neuronal Bcl-xL expression and beta-amyloid-induced apoptosis: relevance to Alzheimer's disease. *72*(4), 1552-1563. doi:10.1046/j.1471-4159.1999.721552.x

Fabiola Olivieri, Ahtiainen, Maarit, Lazzarini, Raffaella, Pöllänen, Eija, & Antonio D. Procopio %J Aging Cell,. (2014). Hormone replacement therapy enhances IGF-1 signaling in skeletal muscle by diminishing miR-182 and miR-223 expressions: A study on postmenopausal monozygotic twin pairs. *13*(5), 850-861.

Roehm PC,Hansen MR %J Current opinion in Otolaryngology & Head and Neck Surgery. (2005). Strategies to preserve or regenerate spiral ganglion neurons. *13*(5), 294-300. doi:10.1097/01.moo.0000180919.68812.b9

Hill RA, HK, Chua, ME, Jones, ER, Simpson, Molecular, Boon WC %J, & Neurosciences cellular. (2009). Estrogen deficiency results in apoptosis in the frontal cortex of adult female aromatase knockout mice. *41*(1), 1-7. doi:10.1016/j.mcn.2008.12.009

Hill RA, S, Pompolo, ME, Jones, ER, Simpson, Molecular, &Boon WC %J, Neurosciences Cellular. (2004). Estrogen deficiency leads to apoptosis in dopaminergic neurons in the medial preoptic area and arcuate nucleus of male mice. *27*(4), 466-476. doi:10.1016/j.mcn.2004.04.012

Liu S, J, Mao, T, Wang, & Fu X %J Molecular Neurobiology. (2017). Downregulation of Aquaporin-4 Protects Brain Against Hypoxia Ischemia via Anti-inflammatory Mechanism. *54*(8), 6426-6435. doi:10.1007/s12035-016-0185-8

Someya S, Prolla TA %J Mechanisms of Ageing & Development. (2010). Mitochondrial oxidative damage and apoptosis in age-related hearing loss. *131*, 480-486. doi:10.1016/j.mad.2010.04.006

Zárate S, T, Stevnsner, & Gredilla R %J Frontiers in Aging Neuroscience,. (2017). Role of Estrogen and Other Sex Hormones in Brain Aging. Neuroprotection and DNA Repair. *9*, 430. doi:10.3389/fnagi.2017.00430

McFadden SL, D, Ding, AG, Reaume, DG, Flood, & Salvi RJ %J Neurobiology of Aging, (1999). Age-related cochlear hair cell loss is enhanced in mice lacking copper/zinc superoxide dismutase. *20*(1), 1-8. doi:10.1016/s0197-4580(99)00018-4

Wu SY, YW, Chen, SF, Tsai, SN, Wu, YH, Shih, YF, Jiang-Shieh, et al. (2016). Estrogen ameliorates microglial activation by inhibiting the Kir2.1 inward-rectifier K(+) channel. *6*, 22864. doi:10.1038/srep22864

Williamson TT, B, Ding, X, Zhu, & Frisina RD %J Aging Cell, . (2019). Hormone replacement therapy attenuates hearing loss: Mechanisms involving estrogen and the IGF-1 pathway. *18*(3), e12939. doi:10.1111/acel.12939

Yune TY, HG, Park, JY, Lee, & Oh T.H. %J Journal of Neurotrauma,. (2008). Estrogen-induced Bcl-2 expression after spinal cord injury is mediated through phosphoinositide-3-kinase/Akt-dependent CREB activation. *25*(9), 1121-1131. doi:10.1089/neu.2008.0544

Cheng W, D, Wu, Q, Zuo, Z, Wang, & Fan W %J International Orthopaedics. (2013). Ginsenoside Rb1 prevents interleukin-1 beta induced inflammation and apoptosis in human articular chondrocytes. *37*(10),

2065-2070. doi:10.1007/s00264-013-1990-6

Cui X, P, Zuo, Q, Zhang, X, Li, Y, Hu, J, Long, et al. (2006). Chronic systemic D-galactose exposure induces memory loss, neurodegeneration, and oxidative damage in mice: protective effects of R-alpha-lipoic acid. *84*(3), 647-654. doi:10.1002/jnr.20899

Tang X, X, Zhu, B, Ding, JP, Walton, RD, Frisina, & Su J %J Neuroscience. (2014). Age-related hearing loss: GABA, nicotinic acetylcholine and NMDA receptor expression changes in spiral ganglion neurons of the mouse. *259*, 184-193. doi:10.1016/j.neuroscience.2013.11.058

Wang Y, & Qin ZH %J Apoptosis : an international journal on programmed cell death. (2010). Molecular and cellular mechanisms of excitotoxic neuronal death. *15*(11), 1382-1402. doi:10.1007/s10495-010-0481-0

Figures

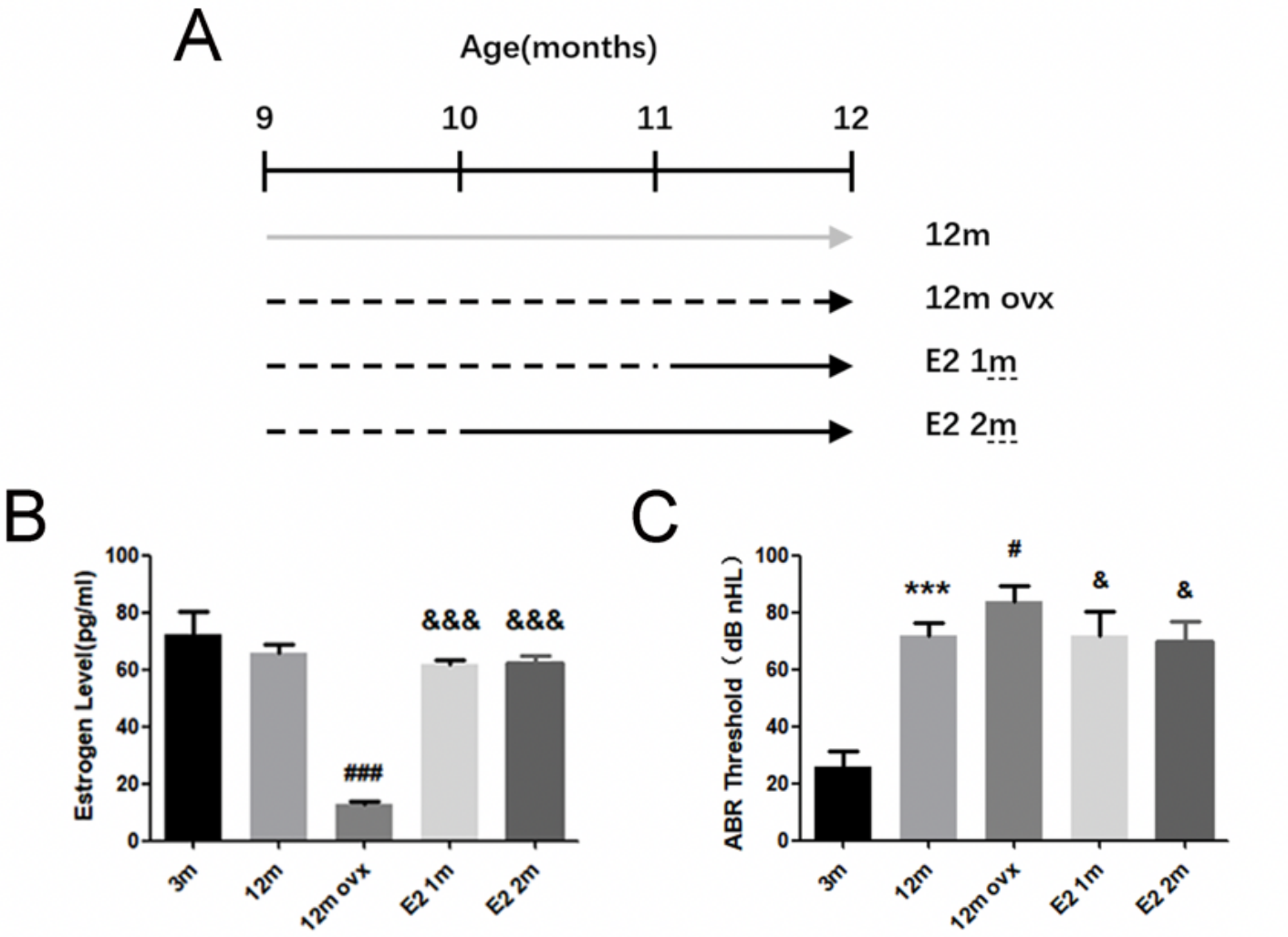

Figure 1

A shows a schematic diagram of estrogen administration. B: Comparison of the estrogen levels in 5 groups of mice. C: Effects of estrogen on the hearing threshold in C57BL/6J mice. The values are expressed as the mean±SD, n=10. For statistical significance, ***P<0.001 versus the 3 m group. #P<0.05, ###P<0.001 versus the 12 m group. & P<0.05 versus the 12 m group. &&& P<0.001 versus 12 m ovx group.

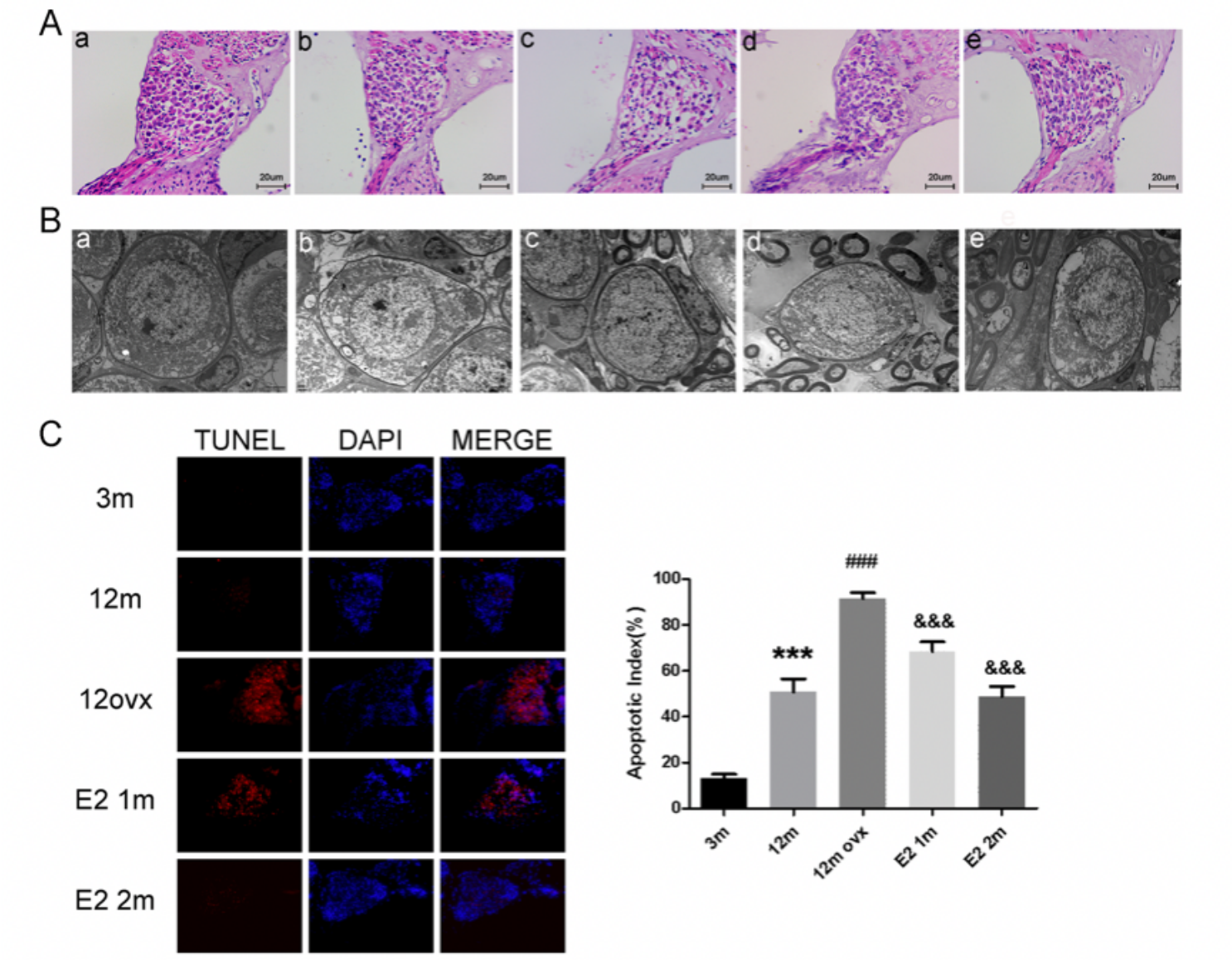

Figure 2

A: Effects of estrogen on the histopathological changes of SGN (400×). B: Effects of estrogen on the damage to spiral ganglion neurons (8000×). C: Effects of estrogen on the apoptosis of cochlear spiral ganglion neurons; cochlear apoptotic cells are labeled with red fluorescence, and DAPI is labeled with blue fluorescence. Comparison of the cochlear spiral ganglion cell apoptosis in each group. The values are expressed as the mean±SD, n=3. For statistical significance, ***P<0.01 versus the 3 m group. ###P<0.001 versus the 12 m group. &&&P<0.001 versus the 12 m ovx group.

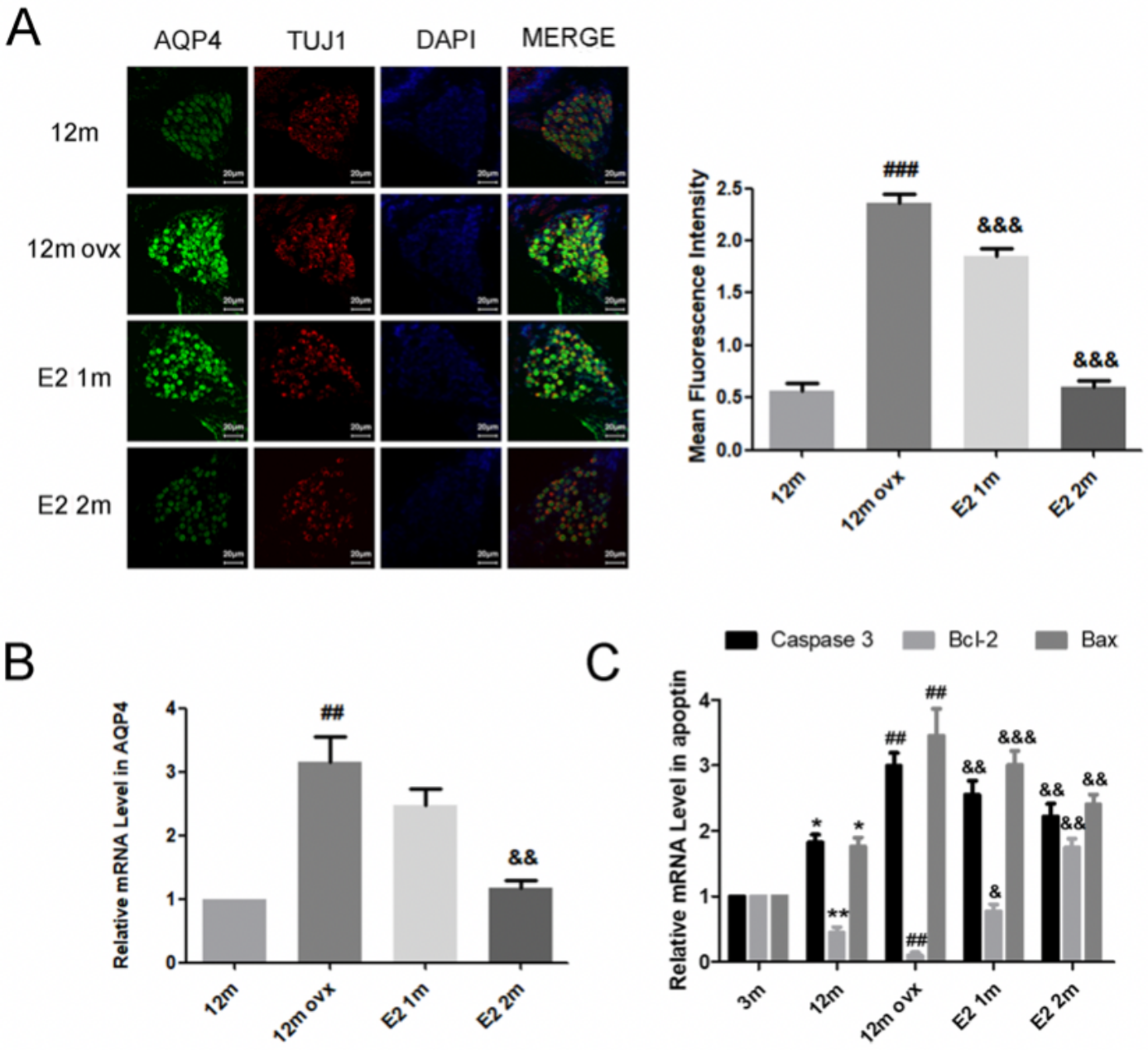

Figure 3

A: Expression of AQP4 in spiral ganglia. A: AQP4 is labeled with green fluorescence, TUJ1 is labeled with red fluorescence and DAPI is labeled with blue fluorescence. Changes in the expression of AQP4 in the spiral ganglion cells. B and C: Effect of estrogen on the gene expression of AQP4, Caspase3, Bax and Bcl-2. B: Changes in the AQP4 mRNA expression in the spiral ganglion in each group. C: Changes in the Caspase 3/Bcl-2/Bax mRNA expression in the mice in each group. The values are expressed as the mean ± SD, n=3. For statistical significance, *P<0.05,**P<0.01 versus the 3 m group. ##P<0.01, ###P<0.001 versus the 12 m group. &P<0.05□&&P<0.01 &&&P<0.001 versus 12 m ovx group.

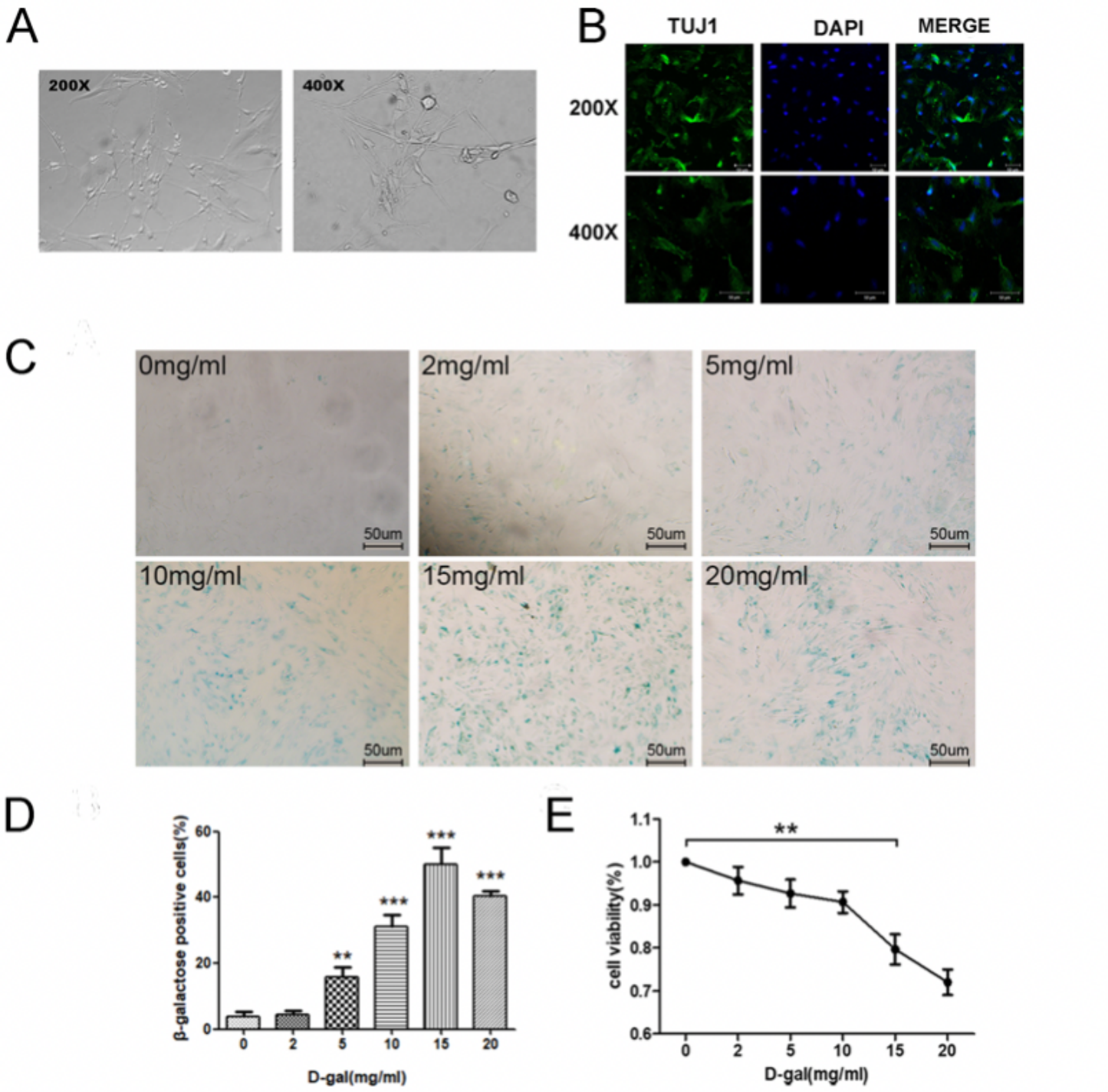

Figure 4

Culture and identification of spiral ganglion cells. A: Primary culture of spiral ganglion cells. B: Expression and location of TUJ1 (green) in primary cultures of spiral ganglion cells. Nuclei were counterstained with DAPI (blue). C: After treatment with D-gal at different concentrations, β-galactose staining was performed. D: β-galactose-positive cell count. E: The CCK-8 kit was used to assess cell viability. All the values are

expressed as the mean ± SD deviation; n=6 in each group, *P<0.05, **P<0.01, ***P<0.001 compared with the con group.

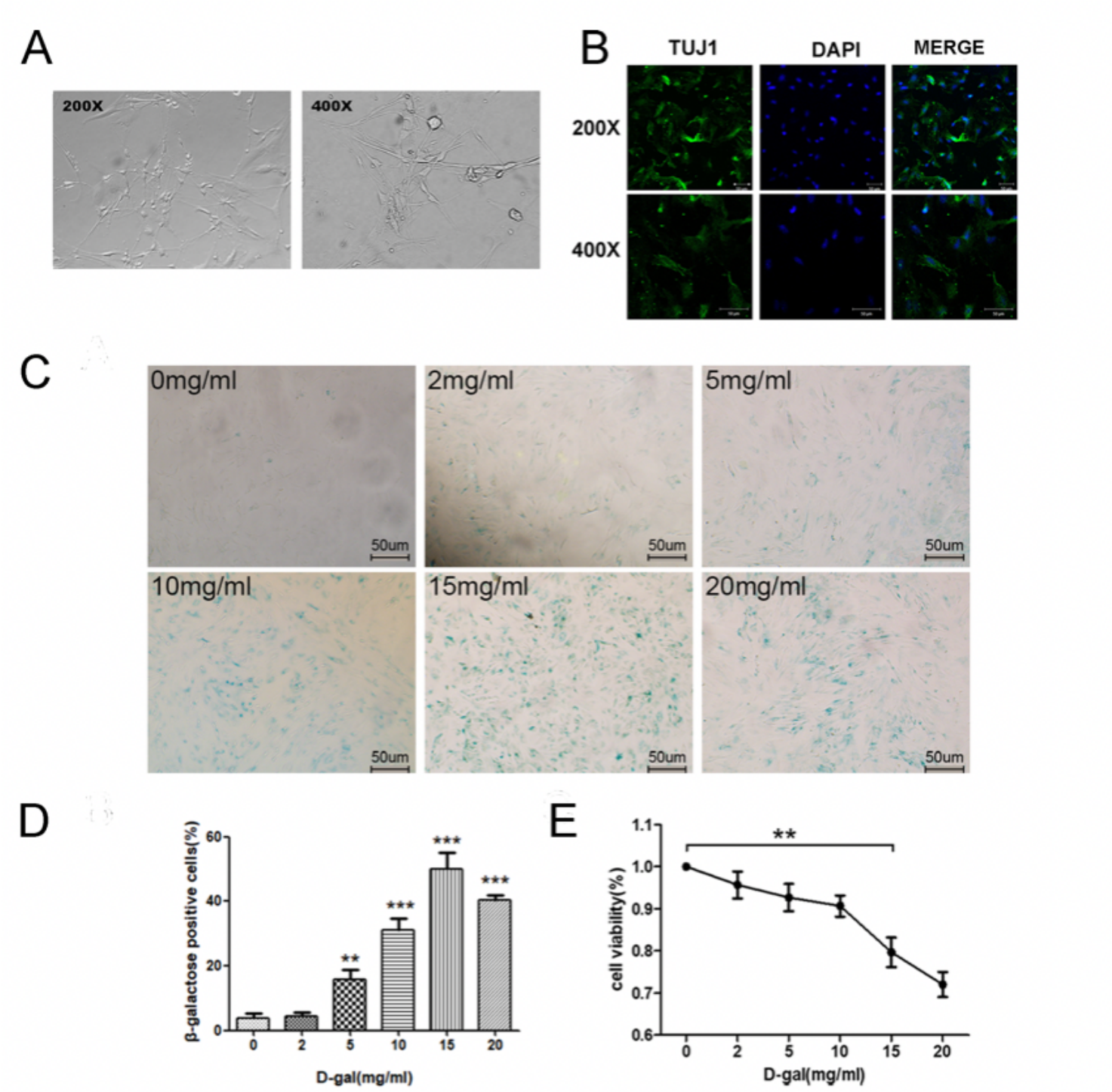

Figure 5

A: AQP4 was labeled with green fluorescence, TUJ1 with red fluorescence, and DAPI with blue fluorescence. Changes in AQP4 expression in the helical ganglion cells. B: Apoptosis of the helical ganglion cells in each group. C and D: Effect of estrogen on the mRNA expression of AQP4, Caspase3, Bax and Bcl-2 in SGCs. C: Changes in the AQP4 mRNA expression in the spiral ganglion cells in each

group. D: Changes in the Caspase 3/Bcl-2/Bax mRNA expression in the mice of each group. All the values are shown as the mean ± SD, n=6. *P<0.0 5, ***P<0.001 versus the SGC group. #P<0.05, ##P<0.01, ###P<0.001 versus the D-gal group.